Interactions of hydrophilic birch wood (*Betula pendula* ROTH) extractives with adhesives for load-bearing timber structures

Max Engelhardt [a,*], Thomas Böger [a], Michael Gigl [b], Chen Meng [b], Viktor Soprunyuk [c], Wilfried Schranz [c], Klaus Richter [a], Antoni Sánchez-Ferrer [a,*]

[a] *Chair of Wood Science, TUM School of Life Sciences, Technical University of Munich, Germany*
[b] *Bavarian Center for Biomolecular Mass Spectrometry, TUM School of Life Sciences, Technical University Munich, Germany*
[c] *Faculty of Physics, University of Vienna, Austria*

ARTICLE INFO

ABSTRACT

This study investigated how water-soluble extractives of silver birch (*Betula pendula* ROTH) wood interact with the most common adhesives used for producing engineered wood products (EWPs), *i.e.*, melamine-urea-formaldehyde (MUF) and one-component polyurethanes (PUR). Therefore, the extractives were characterized via various chromatographic techniques and mass spectrometry. The effects of extractives on the curing kinetics were investigated using rheometry. The impact of extractives on the chemical and mechanical properties of the cured adhesives was investigated with FTIR spectrophotometry and tensile stress-strain measurements, respectively. Moreover, a comparative study on the shear strength of birch wood with and without extractives was performed.

The organic fraction of the water extractives of birch mainly consisted of phenolic glycosides, carboxylic (fatty) acids, and saccharides. The extractives decelerated the curing process of MUF, as observed in a rheological small-angle oscillatory shear experiment using wood substrates as the lower plate. This was indicated by a reduced gel time from 5 to 3.8 h on pristine vs. extracted wood. When measuring MUF on extracted wood, this deceleration was also reached by adding ~1% (W/W) of the isolated extractives into the MUF resin. Similar experiments with PUR showed a slight acceleration when dispersing extract into the adhesive, indicated by a reduction of vitrification time of -0.9 ± 0.3 h per percent of extractives added. However, measurements with pure PUR on pristine and extracted wood showed no significant difference in curing kinetics due to the extractives' limited mobility and solubility in PUR. Both PUR and MUF cured adhesive films showed a reduced stiffness, elastic stress limit and tensile strength in uniaxial tensile stress-strain measurements of adhesive films upon increasing the amount of hydrophilic birch extractives concentration. Comparative standard tensile shear strength measurements on pristine and extracted wood indicate a 7–19% strength increase due to extraction when bonding with MUF, while the bond strength of PUR bond lines was less affected by the extraction procedure.

1. Introduction

Apart from energetic utilization as firewood and use in the pulp and paper industry [1], birch is mainly used in plywood production in combination with phenolic resins [2]. Comparative studies indicated that birch trees generate a significantly higher yield for veneer production compared to beech [3]. Moreover, the first pilot projects of birch-based timber constructions indicate its potential as a building material in timber constructions [4]. With a market share of <1% in engineered wood products (EWPs) production [5] in general, the potential benefits of hardwoods are barely utilized.

The production of EWPs for load-bearing applications, *e.g.*, glued laminated timber (GLT), cross-laminated timber (CLT) and laminated veneer lumber (LVL), requires reliable bonding in a well-controlled

---

process. Due to the wood species' chemical and anatomical characteristics, tensile shear strength and delamination results are not transferable to other wood species, including silver birch [6]. Individual physicochemical characteristics of different wood species, especially the presence of extractives, can have effects on their glueability [7,8]. These include the bond line strength [9–13], the adhesive curing process [9, 14–17], or the mechanical properties of the cured adhesive [9]. Therefore, both the applicable bonding technology and the optimal production parameters for bonding can be affected.

For most wood adhesives, the curing behavior depends on moisture interactions and, therefore, on the adherend's water-related properties: Water-based adhesives like melamine/urea-formaldehyde (MUF and UF) or phenol/resorcinol-formaldehyde (PF and PRF) resins rely on the water uptake of the wood to lose the solvent during the curing process. In contrast, water is a necessary reactant in curing the isocyanate prepolymers in one-component polyurethane (PUR) adhesives, with an optimum molar ratio of 1:2 (water/isocyanate motif) [18]. Insufficient moisture availability due to low wood moisture content results in poor bonding performance [19]. On the other hand, when excessive amounts of water are available from the air during the open time or from the wood, skin formation or increased foaming [20] can occur, leading towards a low crosslinked PUR network and reduced mechanical properties [21]. As a reactant, the water concentration available is naturally governing the curing rate. This sensitivity to the water conditions challenges the observability of the rheological property evolvement during the curing of adhesives under practical conditions of use. Successful implementations of wood-plate setups in rheological equipment by Witt [22] have demonstrated the ability to observe the realistic curing behavior of wood adhesives. Monitoring of the adhesive layer thickness evolution during closed waiting times in a plate-plate rheometer setup of two wooden specimens indicated that wood species impact the curing speed [23]. Consequently, this impacts the rate and amount of adhesive penetration of MUF adhesives. Bockel et al. [24] conducted rheological studies on the effects of common substances in softwood and hardwood extractives on two-component PUR adhesives' curing behavior. An increased curing rate was observed with adding organic acids and polysaccharides, but a lower curing rate was observed when aldehydes or terpenes were added. Similar investigations with MUF adhesives [9] showed significantly accelerated curing by adding aldehydes, terpenes, polysaccharides, as well as simple organic compounds like phenolics or fatty acids. Özparpucu et al. [15] found a prolonged duration to achieve gelation when acidic extractives from chestnut or gallic acid are added to MUF adhesives. This ambiguity confirms older literature reviews by Hse & Kuo [7], which also found retardation – due to water extractives in teak and red oak – as well as acceleration – in the case of ethanol extractives of white oak – of acid-catalyzed curing of UF resins.

Extractives can contain substances that can covalently integrate into the adhesive's polymer structure during curing [25,26]. Others remain unbound but may inhibit or catalyze the curing process [9]. The polymer networks' cross-linking density or segmental molecular weight can be affected in both cases. This can change the adhesive's mechanical properties, reflected in Young's modulus (stiffness), yielding behavior (elastic stress and strain limits), and strength values. Determining those properties is possible ex-situ on cured adhesive films [27], applying sample preparation and tensile measurement techniques suitable for the respective curing mechanisms [28].

Various studies are available on the extractives composition of birch wood, however, no studies were identified, where water as a solvent, which could also be considered a simple extraction pretreatment method without additional solvent chemicals required. Instead, birch related studies mostly used non-polar solvents such as light petroleum [29,30] and polar solvents like acetone [31,32] or methanol [1,33,34], yielding differing results on extractives compositions, containing fatty acids and its' esters, glycolipids, terpenoids (triterpenes, steroids, steryl esters), polyphenols (lignans, flavonoids, condensed tannins) and phenolic

glycosides.

Since the xylem chemistry of different tree species [30] and even within birch species [35] varies considerably, the introduced phenomena need to be addressed for wood species individually. Reviewing available literature, no investigations were found considering birch wood's specific characteristics on adhesive curing. Regarding the mechanical properties of cured adhesives films, no prior studies were found on the effects of extractives, birch or otherwise.

For producing glued laminated timber (GLT), about 50% of the companies use water-based melamine-urea-formaldehyde (MUF) and 35% use one-component polyurethane (PUR), according to a survey among producers in Central Europe [5].

The present study investigates the fundamental interactions between both of these adhesives and the water-soluble hardwood extractives of silver birch silver birch (*Betula pendula* Rotи; Syn.: *Betula verrucosa* Ehrh.), which is one of the more prevalent *Betulaceae* species with superior timber quality [36] compared to downy birch (*Betula pubescens* Ehrh.). These interactions include the effects on curing behavior and the final adhesives' properties as well as bond strength. Since water-insoluble compounds are mostly inert, this study focuses on water-soluble extractives and their interaction with the common adhesives used for the production of GLT, *i.e.*, MUF and PUR. Determining how birch wood extractives can affect the curing behavior and the final adhesive properties shall give insights for a optimization of birch wood bonding for EWP.

2. Experimental section

2.1. Materials and preparations

Boards of defect-free wood (straight-grained, knot- and pith-free, and without discolorations) silver birch (*Betula pendula* Rotи) from Lieska (Finland) with a density of 600 ± 35 kg/m^3 (average $\pm$ standard deviation) was used in this study. Unless otherwise stated, wooden material and wood samples were stored and used in standard air climate of 20 °C and 65% relative humidity (RH).

Since, for some experiments, comparative measurements with pristine and extracted wood samples had to be conducted, boards of 15×35 cm were planed to 5.2 mm, and half of the boards were subjected to an extraction process. Therefore, the boards were submerged in deionized water at 20 °C using glass basins and glass fixtures with a solvent-to-solute ratio of 10:1 (V/V) for 4 d, with a solvent exchange after every 2 d. After the extraction, all boards (including untreated) were reconditioned to 20 °C/40%-RH and subsequently to 20 °C/65%-RH – reaching the final moisture conditions in adsorption process – to prevent sorption hysteresis effects [37].

In order to isolate sufficient amounts of the hydrophilic and amphiphilic extractable compounds and create adhesive–extractive mixtures, a specific particle fraction of birch wood was produced. Therefore, a mixture of equal amounts of 1 cm^3 blocks of birch wood (sampled equally from both inner and outer log regions of 10 different boards) and dry ice was coarsely milled (0.75 mm screen) in a cross hammer mill to refine the wood without thermic exposure before re-equilibrating at standard air conditions of 20 °C/65%-RH, and separating a mesh size fraction of 125 μm $< \xi <$ 315 μm with a vibratory sieve shaker (AS 200, Retsch GmbH). The extraction was performed with deionized water (25 g dry wood per L H$_2$O) at 20 °C – as hot water extraction would lead to extraction compounds, which are not dissolved at the room temperature conditions representative for bonding EWPs like GLT – for 7 d under constant stirring. After filtering the solution with a P 4 fritted glass filter (pore size index 10–16 μm), it was concentrated with a rotary evaporator (35 °C and 40 mbar) before removing the solvent by lyophilization. The residual solid powder of extractives was stored in dry conditions in a deep freezer for further use and within a desiccator filled with silica gel when needed in the laboratory.

As a MUF adhesive, Kauramin 683 resin with hardener Kauramin

688 (BASF AG in Ludwigshafen, Germany) was used with a mixing ratio of 100:25 (W/W); as a PUR system, PURBOND® HB S309 (Henkel & Cie. AG Sempach Station in Sempach-Station, Switzerland) was chosen.

2.2. Chemical analyses

The isolated extractives were quantified gravimetrically, and the ash content was determined via combustion in a muffle furnace at 550 °C for 1 h. The extractives were further analyzed via gas chromatography coupled with a mass spectrometer (GC-MS), ultra-high performance liquid chromatography coupled with electrospray ionization time-of-flight mass spectrometry (UHPLC-ESI-TOF-MS) and a liquid chromatography (LC) sugar analyzer. The analyses aimed to obtain information about the extract's chemical composition, thus allowing better conclusions about their interactions to be drawn. Moreover, the adhesive films were analyzed with Fourier-transform infrared spectrometry in attenuated total reflection mode (ATR-FTIR) to observe any chemical changes in the polymers due to the presence of extractives.

For an untargeted GC-MS analysis, 200 μL DMF was used to dissolve 1 mg of dry extract and heneicosanoic acid (CAS No: 2363-71-5) as an internal standard for semi-quantitative analysis. The solution was derivatized using 50 μL of a BSTFA/TMCS silylation reagent (CAS No: 25561-30-2) and applying reaction conditions of 80 °C for 60 min. For an extract sample, two vials of derivatized solution were produced for repeat determination and analyzed twice for verification. A 5975C VL MSD and 7890A GC gas chromatograph (Agilent Technologies, Inc., Santa Clara, USA) equipped with a 250 μm by 30 m SGE™ BPX5 column were used for the analysis of 1 μL injection volume (split ratio 1:30) by applying a temperature gradient of 10 K/min from 100 °C to 320 °C. The temperatures at the interface and injector were 250 °C and 320 °C, respectively.

Peaks in the total ionization chromatogram (TIC) were selected with a minimum threshold of 0.2% of the maximum peak area. The MS spectra of the peaks were identified using a probability-based matching algorithm [38] and spectral database (NIST/EPA/NIH Mass Spectral Library NIST 14 and NIST Mass Spectral Search Program V2.2) via the MSD ChemStation software. The library search results were manually reviewed to remove implausible or inconclusive library hits. The amounts for identified compounds are given following a semi-quantitative method after correcting molar masses for silylation weight gain. Linearity calibration was conducted using only internal standard data (heneicosanoic acid). No response factors were applied.

As saccharides are challenging to differentiate in untargeted GC-MS, free sugar contents of the extracts were analyzed with a ZA 3000 liquid chromatography sugar analyzer (Laborservice Onken GmbH, Gründau, Germany). Here, boric acid buffers are used to form negatively charged borate-sugar complexes with high specific column interaction in a stepped elution process. The device is optimized for detection of multiple monosaccharides and cellobiose *via* respective external standard solutions. Therefore, prior to the measurements, gentle hydrolysis [39] of the extract is performed after adding 20 mL of 2 mol/L trifluoroacetic acid to 20 mg of extract (hydrolysis method I) to break down the sugars into their monomeric constituents (60 min at 102 °C). An alternative hydrolysis treatment [40] is performed on 20 mg of the extract with 7.5 g of trifluoroacetic acid at 102 °C for 20 min and another 60 min after adding 12.5 mL of water (hydrolysis method II). The respective saccharide concentrations measured on the hydrolysate yielding the higher values were reported. The LC was calibrated to perform a targeted analysis of cellobiose, rhamnose, mannose, arabinose, galactose, xylose and glucose.

A Nexera UHPLC system (Shimadzu Corp., Kyoto, Japan) with a reversed-phase column (Kinetex XB-C18, 2.1 × 100, 1.7 μm) coupled with a Q-TOF mass spectrometer (TripleTOF6600, Sciex, Darmstadt, Germany) was used for untargeted metabolomics analysis of the extractives via UHPLC-ESI-TOF-MS to extend the detection of compounds to a higher molecular weight range. For analysis, 1 mg/mL dry extract

powder was dissolved in acetonitrile-water and separated via gradient elution using 0.1% formic acid and 0.1% formic acid in acetonitrile as eluents. Information-dependent acquisition (IDA) and negative ionization mode were used for MS data collection.

The "msconvert" tool from ProteoWizard [41] was used to convert raw files to mzXML (de-noised by centroid peaks). The bioconductor/R package xcms was used for data processing and feature identification. More specifically, the matchedFilter algorithm was used to identify peaks (full width at half maximum set to 7.5 s). Then the peaks were grouped into features using the peak density method [42]. The area under the peak was integrated to represent the abundance of features. Missing values were imputed by integrating the intensity area according to the features' retention time and mass range. To annotate features with names of metabolites, the exact mass and MS2 fragmentation pattern of the measured features were compared to the records in the public MS/MS spectra in MSDIAL [43], referred to as MS1 and MS2 annotation, respectively. We further performed molecular structure estimation data via Sirius & FingerID software [44] to select plausible compounds and assign basic chemical classes. Determining the composition of chemical compound classes, instead of identifying exact molecular structures, was considered adequate for the purpose of this study, given the wide variety of similar compounds.

The infrared spectra of adhesive films, produced without and with varying extractive concentrations, were analyzed with a Nicolet iS50 FTIR Spectrometer (Thermo Fisher Scientific Inc., Waltham, USA) in the wavenumber interval from $\bar{v} = 4000$ to $650\ cm^{-1}$, equipped with an ATR monolithic diamond (GladiATR by PIKE Technologies, Madison, USA). Before measuring every film, a background measurement was conducted for subtraction. Averaged spectra were recorded by conducting 16 scans with $0.5\ cm^{-1}$ resolution at ten random positions of the film surface (160 scans total) after conditioning at 20 °C/65%-RH. Normalized spectra were calculated by scaling to matching areas.

2.3. Rheological experiments of isothermal curing

Based on experiences from studies with similar methodologies [22, 23,45,46], an adapted method of Small-Amplitude-Oscillatory Shear (SAOS) experiments was developed. The developed method mimics the conditions of adhesives in a wood bond line while monitoring the curing in a time-sweep rheological measurement. The experiments were conducted with an MCR 301 rheometer (Anton Paar Group AG, Graz, Austria) in a plate-plate configuration using disposable plates (25 mm diameter) of stainless steel and aluminum for MUF and PUR, respectively. For the static lower plate, a mechanical fixture to mount rectangular plates of wood with a radial cut surface of 35 × 35 mm was installed. These plates were produced from pristine wood as well as wood previously exposed to the above-described extraction treatment. In order to create sufficiently flat surfaces for the shear measurement, the wood plate surfaces were sanded with up to 500-grit sandpaper.

Comparative experiments were conducted with pure MUF and PUR adhesives on pristine and extracted wood surfaces. However, when bonding wood, extractives diffusion initiates in a sub-surface region where the adhesive penetrates the wood structure by wetting, capillary action and pressing force – the interphase [24]. Since the rheological setup is pressureless and is designed to measure the adhesive's properties between the two plates, instead of inside the interphase, a workaround was used: Adhesive–extractives mixtures in varying concentrations were applied to extracted wood surfaces (bottom plate) to assess the effect of extractives on the curing behavior in a more controlled way.

The dry extractive was added to the adhesive in a strictly timed manner: The duration after weigh-in-of precise amounts (1712 MP8 analytical balance with 0.01 mg resolution, Sartorius AG, Göttingen, Germany) of resin (and, if applicable, hardener), as well as dry extractive powder and the start of the experiment, was kept constant. During the first minute, the adhesive and extractives were thoroughly

dispersed, followed by applying the mixture on the lower plate and lowering the upper plate until minute 2:00 before trimming the squeeze-out and starting the sequence at 3:30 min.

The initial gap size was set to 0.28 and 0.14 mm for MUF and PUR, respectively, corresponding to the respective amounts per area applied (350 and 160 g/m^2) according to the supplier's recommendations. When measuring the solvent-free PUR, the gap was kept at a constant thickness to avoid gap expansion from the CO_2 pressure buildup. Measurements on MUF were conducted by controlling axial force on the upper plate to a threshold of <0.1 N by varying the gap thickness and, thereby, adapting to the shrinkage of the adhesive during curing.

The temperature and humidity conditions during the measurements were controlled with a purgeable enclosure: 20 °C/65%-RH for measuring MUF and 20 °C/< 2%-RH for measuring PUR because dry air conditions for experiments on PUR are necessary to avoid additional curing at the gap opening. In order to avoid water loss of the wood samples to the dry environment during PUR measurements, the wood plates were encapsulated with a diffusion barrier (aluminum tape), only leaving the circular area of 26 mm diameter uncovered, where the adhesive and upper plate was positioned. The dry airflow was set to 300 L$_N$/h in the initial experimental phase for purging and reduced to 50 L$_N$/h after 10 min. Measuring PUR adhesive in these conditions prevents accelerated curing of the adhesive at the air-exposed peripheral gap surface, restricting water availability to the wood equilibrium moisture content in the lower plate.

The measurement sequence consists of a looped frequency sweep in the range of 1–10 Hz with a duration of 90 s, repeated 720 times, resulting in an 18 h time-sweep experiment with multiple frequencies (alternatively, multi-wave modes using Fourier transform mechanical spectroscopy [47] can be applied). The shear deformation was kept constant in the linear viscoelastic regime (LVE) at 0.1% strain value.

The time-resolved frequency dependence of the loss tangent was analyzed to determine when percolation of the polymer network occurs using the following relation: While the loss factor (tan δ) is positively correlated with frequency in the liquid state and negatively correlated after gelation, it is frequency-independent at gelation. This is because both the storage and the loss modulus follow a power-law frequency function with the same relaxation exponent [48]. This approach is more reliable in determining gelation than the commonly used crossover criterion, G' = G" (when a solid-like behavior appears, G' ≥ G", coming from a liquid-like behavior, G' < G"), which is valid only for end-linking polymer networks, which are stoichiometrically balanced [49]. An automated, algorithmically robust way to determine the gel time was realized: First, all results of the frequency sweeps were detrended by linear interpolation of the current, prior and the following sweep and predicting the sweep results at its average cycle time by interpolation. This step effectively eliminates the variance due to the advancement of the curing during each frequency sweep. The gel time (t$_{gel}$) – when the tan δ shows constant values, independent of frequency – was then determined by identifying the local minimum of the variance s^2 of the detrended loss factor tan δ as a function of frequency f. In Figs. SI–2, this process is shown in a graphical representation.

Furthermore, the time needed to transition to a glassy state or vitrification time (t$_{glass}$) was determined by a loss modulus (G") peak in the solid state. The relaxation exponent at the gel time $n_c = 2/\pi \bullet \tan^{-1} G''/G'$ [50] was calculated. The relaxation exponent n_c describes the relaxation behavior of the critical gel, which follows a power law $G(t) = St^{-n}$ (with a strength factor S) [49]. It is limited to values between 0 (limit case for elastic gel) and 1 (limit case for viscous gel), and is indicative of the stoichiometric conditions (lack or excess of hardener) of the curing process [51]. Lastly, a simple viscosity criterion for the onset of curing t$_\eta$ was evaluated as the time when the dynamic viscosity reached η* >100 Pa s [15].

2.4. Mechanical analysis of cured adhesive films

Cured films of both adhesives were produced at 20 °C/65%-RH by casting the adhesive or adhesive–extractive mixture with a doctor blade at a constant speed of 0.5 m/min on 100 μm PET sheets. The blade gap was 200 μm and 100 μm for MUF and PUR, respectively. The resulting cured films had an average thickness of 100 μm and 58 μm, respectively. After 48 h, the tensile samples were prepared by removing the substrate sheets and cutting rectangular strips of 6 × 70 mm with a die cutter in a pneumatic press and stored for 100 d to ensure fully cured conditions.

Limited by their solubility and preparation time, films with extractive concentrations of 0.05%, 0.1% and 0.2% (W/W) were produced. In the case of MUF, films with extractive concentrations of 0.5% and 1.0% could also be produced.

Attention was paid to reproducible measurement of the film thickness, which in recent round-robin tests proved to significantly influence measurement uncertainty in tensile tests on thin films [52]. It was measured and averaged at five equidistant positions along the length of the specimens using a digital length gauge (MT 101 M, Dr. Johannes Heidenhain GmbH, Traunreuth, Germany). The length gauge applied a motor-controlled contact force of 0.7 N, was rated at an accuracy of ±1 μm and was equipped with a flat probe (diameter 14 mm) on a self-leveling support.

Engineering stress-strain curves were constructed by analyzing the film samples in tension at a strain rate of 1%/min using a universal test machine equipped with an S2 100 N load cell (Hottinger Baldwin Messtechnik GmbH (HBM), Darmstadt, Germany) and a WA50 inductive displacement gauge (HBM). For the fixation of the specimens, a parallel clamping system with a 60 mm initial free length and thin rubber padding was used. The Young's modulus of the specimen was evaluated by linear regression in the engineering strain interval from 0.05% to 0.25% [53]. The yield point was identified by the offset method (proof stress) at 0.2% plastic deformation [54].

The adhesive films' temperature-dependent softening was measured using a TMA 40 thermo-mechanical analyzer (Mettler-Toledo International Inc., Columbus, USA) with a spherical probe tip (Ø 6 mm). The probe contact force was 0.15 N. The temperature program was a constant gradient of 2 K/min in the range of 25 °C–200 °C. To increase the signal, stacks of ten film layers (cut-outs of 5 mm by 5 mm) were used as specimens. Glass transition temperatures were evaluated with Mettler software STARe SW 14.00 using its midpoint criterion.

Dynamic mechanical analysis (DMA) temperature- and frequency-sweep experiments were performed in tension geometry to measure the temperature and frequency behaviors of cured PUR and MUF samples using a Diamond DMA and DMA 8000 (PerkinElmer Inc., Wellesley, USA), respectively. The temperature sweeps were conducted at a heating temperature rate of 2 K/min in the temperature region from −115 to 115 °C at frequencies of 0.1, 1, 10, and 70 Hz under N$_2$ atmosphere. The frequency sweeps were conducted at 20 °C in the range from 0.1 to 60 Hz at different RH-values, *i.e.*, 0, 65 and 90%-RH.

2.5. Tensile shear experiments

A simple comparative measurement campaign was conducted to contrast tensile shear strength (TSS) and wood failure percentage (WFP) of pristine versus extracted birch wood lap joint samples. Sample preparation with MUF and PUR adhesive followed the common standard procedure [55], using pristine and extracted birch wood, as described above. The surfaces were sanded (200-grit) and cleaned with pressurized air before gluing. The processing parameters for bonding (conducted at 20 °C/65%-RH) can be found in Tables SI–1.

The samples of each wood and adhesive type combination were grouped into four batches of eighteen samples and subjected to the treatments A1, A2, A4 and A5 as defined in EN 302-1 (listed in Tables SI–2). The lap shear specimen geometry and the cutting pattern with respective specimen treatments are shown in Figs. SI–1. The

measurements were conducted with a universal test machine (Test 112, Test GMbH, Erkrath, Germany) equipped with wedge clamps (diamond grips) and a 5 kN force load cell (ISO 376 accuracy class 0.5, Type 307 by Test GmbH).

3. Results and discussion

3.1. Chemical characteristics of extractives

To explain the interaction phenomena of the extractives with the adhesives, knowledge about their chemical nature and composition was required. Therefore, untargeted chromatographic methods (GC-MS and UHPLC-MS) and targeted liquid chromatography for common sugars in wood (LC sugar analyzer) were applied.

The extractives solution pH prior to isolation was 5.6 – which can be affected by dissolved CO_2 during extraction – and gravimetric quantification of the isolated dry extractives yielded water-soluble extractive contents of the used birch wood of 1.4% (W/W) per dry wood mass. The ash content of the birch extractives was determined to be 32% (W/W) of the total extractives, resulting in 0.45% (W/W) inorganic water-soluble per dry wood mass. This is in line with literature data on ashes in European birch wood of 0.3–0.4% (W/W) [56].

The total sugar content detected and analyzed by LC sugar analysis was 8% (W/W) of the extractive. The saccharide fraction mainly consists of glucose (45 mg/g) and xylose (15 mg/g), as well as minor amounts of arabinose, galactose, mannose and rhamnose (5.0, 4.3, 3.8, and 2.7 mg/g, respectively). The remaining fraction of detected oligosaccharides in LC sugar analysis indicates that the hydrolysis methods applied could not entirely convert all saccharides and glycosides into monomeric components. More detailed results can be found in Tables SI–4.

The organic compounds detected with GC-MS (list of most abundant compounds in Tables SI–4) were also identified mainly as monosaccharides (71% (W/W) of identified compounds) and carboxylic acids (24% (W/W) of identified compounds), in a molecular weight range of ~100–200 Da. As per peak area, 90% of the considered compounds in the chromatogram could be identified, while 10% yielded inconclusive spectral data. However, based on the abundance of internal standard and the extractive peaks, the total amount of identified compounds was estimated to correspond to only 10–20% of the total sample mass. Therefore, a significant portion of high-molar mass fractions, e.g., fatty acids, lignans or phenolic glycosides, was not detectable by the applied GC-MS method.

Untargeted analysis via UHPLC-ESI-TOF-MS (Fig. 1, Tables SI–5) revealed the expected higher molar mass fractions. Those include phenolic glycosides, the largest compound class, identified by qualitative assessment via peak area (total ion current (TIC) abundance). Of the total abundance, 61% (96 compounds, including lignan glycosides and flavonoid glycosides) is in a molar mass range of predominantly 400–600 Da. Amphiphilic fatty acids and conjugates (oxidized fatty

acids increase compatibility with polar solvents) are the second most prominent compound class identified, with 24% of total abundance (32 compounds). The abundance percentage of saccharides is 5.4%, which is lower than the LC sugar analyzer results. However, the sugar analyzer analysis included hydrolyzed sugars fractions, which can be part of the other glycosidic compounds. Other minor compound classes are glycolipids, glycerolipids, polyphenols/lignans, and phenolics, representing 10% of the total abundance.

Regarding possible adhesive interactions, aromatic compounds (here, phenyl glycosides, polyphenols/lignans, and simple phenolics) can react via electrophilic substitution with the formaldehyde fraction in the acidic milieu of the MUF resin. In parallel, glycosides and saccharides might work as cross-linking agents [57–59]. Regarding the PUR adhesive interactions, all detected organic compounds could react to some extent via hydroxyl groups with isocyanate moieties in the adhesive. Here, they could form the corresponding carbamate/urethane linkages, leading to cross-linking, chain-extending or chain-ending effects, depending on the number of reacting hydroxyl groups per organic molecule. Adding an excess of crosslinkers can result in defects in the adhesive network [60], i.e., dangling chains and chain extension. Moreover, acidic compounds are expected to increase the curing reaction rate of the PUR adhesive [61].

Non-reacting additives can be considered diluents, therefore having a decelerating effect on curing reactions. Non-reacted fractions of extractives in either adhesive can cause physical disruptions in the polymer networks, which reduce strength and stiffness properties [62] and can act as plasticizing agents [63]. The plasticization can be amplified by the hydrophilicity of extractives, introducing an increased water content into the polymer network in cured equilibrium conditions. The inorganic mineral fraction of the extractives is also expected to be hydrophilic salts, contributing to this effect. However, at the same time, it might reinforce the network as fillers due to the presence of organic/inorganic interface interactions in hydrophobic adhesives, e.g., PUR – this is not the case for waterborne adhesives where inorganics are dissolved at the ionic level.

3.2. Chemical characteristics of cured adhesive-extractives mixtures

The infrared spectroscopy experiments on cured adhesive films revealed only minor differences in the absorbance spectra of both adhesive types concerning the studied extractive concentration range. The FTIR spectra of MUF films show absorption peaks in the fingerprint region at ca. 1547, 1486 and 1347 cm^{-1} that decrease with increasing extractives concentration. The 1547 cm^{-1} peak is associated with secondary amide (-HN-CO-) from the urea motif. The peaks at 1486 cm^{-1} (-CH$_2$-) and 1347 cm^{-1} (>N-CH$_2$-N<) of MUF adhesive films are associated with methylene bridges [64,65]. They form from formaldehyde reactions with melamine/urea or its reaction with aromatic compounds in the extractives. The decrease in intensity of those peaks indicates that
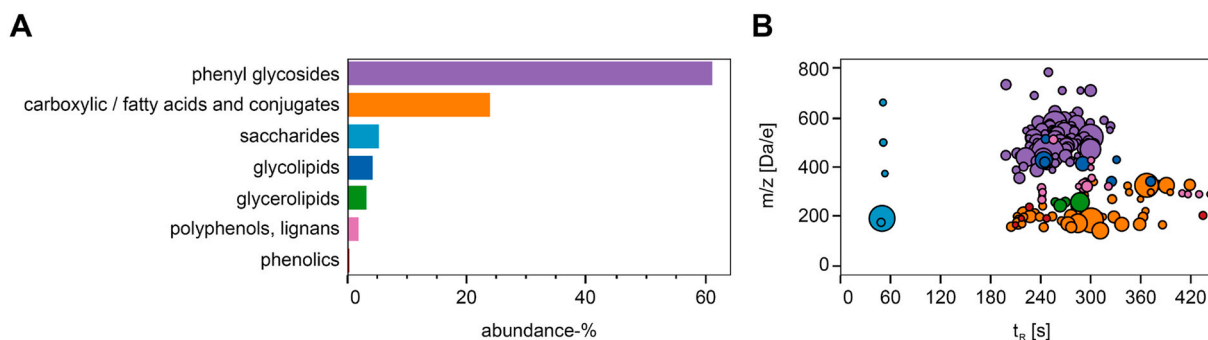

Fig. 1. Compound classes identified by untargeted metabolomic analysis via UHPLC-ESI-TOF-MS with reversed-phase column and negative ionization mode. A) fraction of total abundance for chemical compound classes; B): mass-to-charge ratio (m/z) over retention time of reviewed compounds (dot size indicates abundance/peak area).

those vibrational modes belong to the polymer adhesive compounds (dilution effect). For a better understanding of the curing process in MUF adhesives and to distinguish between the peaks from the starting materials and the ones corresponding to the formed motifs, FTIR spectra for the MUF resin and the hardener, together with the cured MUF adhesive, are shown in Figs. SI–3A.

The averaged FTIR spectra of PUR films show a peak at around 1078 cm^{-1}, which decreases with extractives concentration. This peak is associated with the -C-OR-stretching of hydroxyl (R = H) or ether (R = C) groups [66] coming from the polymer backbone of the PUR adhesive, *i.e.*, polyglycols. Moreover, peaks at 1660, 1538 and 1508 cm^{-1} also decrease with adding extractives. Those peaks are associated with the formation of substituted urea groups [67,68] which correspond to the amide I (-HNC=O) and amide II (-HN-CO-) in urea motifs formed during PUR curing with water. The decrease in the peak intensity indicates that hydroxyl moieties in the extractives did not react with the isocyanates

from PUR to offset the dilution effect. This is due to the faster reactivity of water molecules with isocyanates than aliphatic or aromatic alcohols in the extractives. The decrease of the strong PUR peak at 1078 cm^{-1} is likewise interpreted as a dilution effect. Individual peaks of extractives are strongly masked by the adhesives at the studied concentration levels. FTIR spectra for the PUR prepolymer and the cured PUR adhesive are shown in Figs. SI–3B.

Fig. 2A and B give an overview of the FTIR spectra of pure MUF and PUR and with extractives. Fig. 2C and D shows the absolute deviation of spectra with varying extractive concentrations to the reference spectra (no extractives), with grey bands indicating the positions of the discussed peaks. Fig. 2E and F shows the linearity of the peak absorbance changes as a function of extractives concentration with negative correlations corresponding to peak signals coming from the cured adhesive matrix.

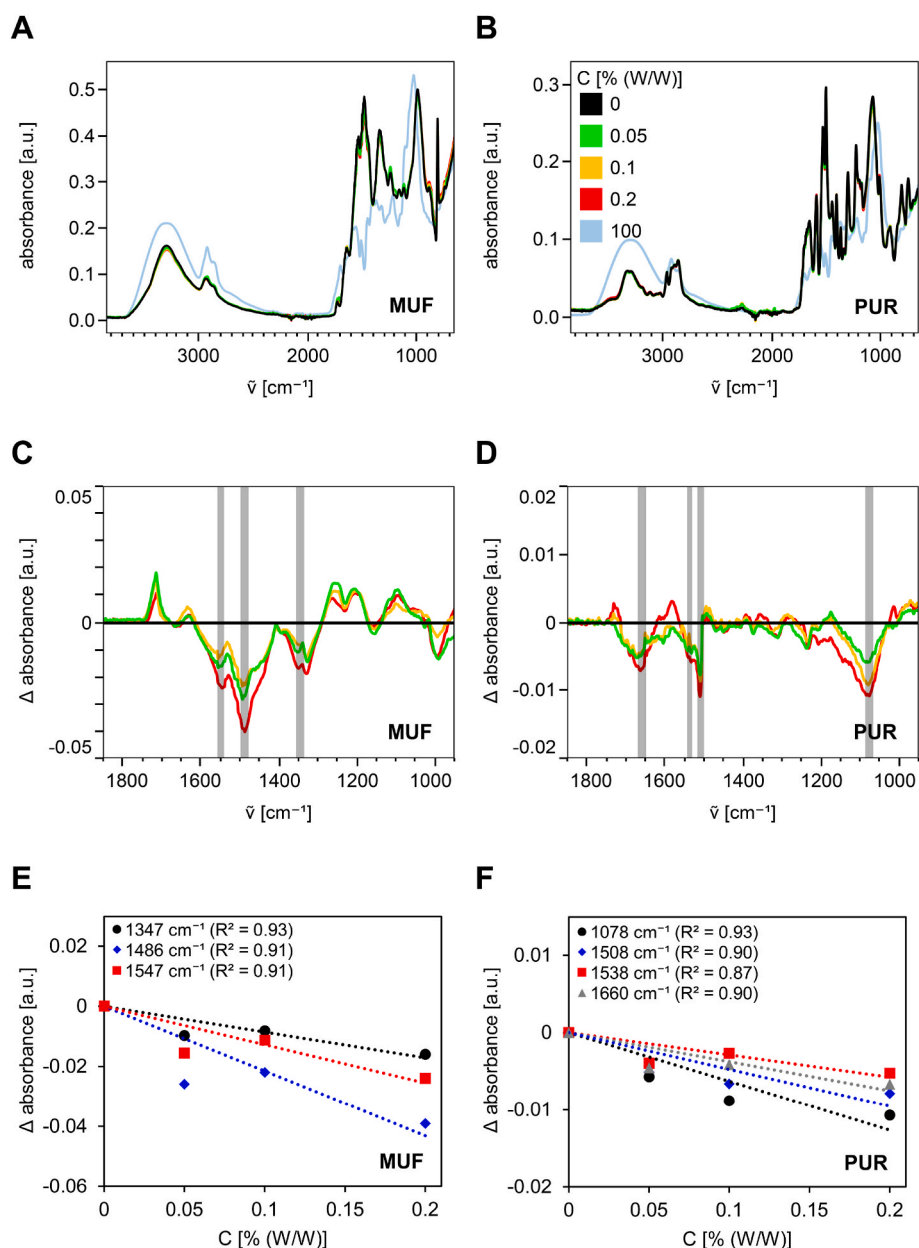A general interpretation of the absorbance spectra of these adhesive

Fig. 2. Normalized FTIR–ATR spectra of adhesive films (A: MUF; B: PUR) with varying concentrations of silver birch extractives. Absorbance deviation to the reference spectrum (pure cured adhesive = 0% (W/W) extractive addition) (C: MUF; D: PUR). Change in absorbance peak heights at wavenumber values correlating with extractives concentration in the adhesive films (E: MUF; F: PUR).

types can be found elsewhere [69,70].

3.3. Rheological experiments of isothermal curing

The curing kinetics are relevant characteristics to be determined to choose optimal processing parameters or select the appropriate adhesive formulation and subsequently assure good bonding results. Understanding the nature of the extractives' influence is also essential to develop mitigation treatments. Isothermal time-sweep measurements (small-angle oscillatory shear mode) of adhesives with various concentrations of birch extractives were conducted with a plate-plate setup. For the lower plate material in the rheometer, wood plates (radial cut and sanded surface) were used to mimic curing conditions in the bond line. Furthermore, experiments on pure adhesives using pristine and extracted birch wood plates were performed for direct comparison.

Fig. 3 shows the curing process for pure MUF and PUR adhesives on extracted birch wood. The progression of the storage and loss modulus (G' and G", respectively) in Fig. 3A and B shows the formation of a soft solid when both moduli cross (t_{cross}, dotted line), and a glass formation when G" peaks (t_{glass}, dashed line). The loss factor ($\tan \delta$) is shown in Fig. 4C and D for the lowest frequency (1 Hz), highest frequency (10 Hz) and the geometric mean ($\sqrt{10}$ Hz). The same figure presents the t_{cross} at the respective frequencies (dashed lines) and the occurrence of the gel point (t_{gel}, white dot with black circle), evaluated by the local minimum of loss factor variance (Figs. SI–4D to Figs. SI–19D).

During the experiments, both adhesives transform from liquid (G" > G') to solid (G' > G") conditions forming first a gel (t_{gel}) and finally a rigid solid (t_{glass}). MUF shows a continuous increase in the intrinsic viscosity (Figs. SI–4B to Figs. SI–13B), but PUR adhesive undergoes a transitory phase of solid-like (G' > G") behavior within the first 0.5 h of curing with a reduction in measured viscosity (Figs. SI–14B to Figs. SI–19B) due to the initial foaming and pressure built-up. This pressure built-up (Figs. SI–20B) due to the formation of CO_2 pores also coincides with a transient crossover of G' and G" in this initial phase, which reverses after pressure release at ~ 0.3 h.

It can be seen that the crossing method (see lines indicating crossover of loss factor to ≤ 1 in Fig. 3C) underestimates the cross-linking state of the adhesive considerably for MUF, as the evaluated gel point occurs at an earlier time. The relaxation exponent of MUF at the gel time is $n_c = 0.64 \pm 0.03$, with no significant correlation to the extractives concentration, indicating that the stoichiometric conditions of the curing process are not affected to a considerable extent. On the contrary, the gel time and the crossover time are more similar in the case of the PUR adhesive (Fig. 3D). This coincides with an average n_c of 0.52, close to the model assumption of 0.5 for the crossover method.

Regarding the measured shear moduli (Fig. 3A and B), while approaching the almost cured state (G'-plateau), the viscoelastic properties of the wooden substrate become a more significant source of error. While they can be neglected in the initial phases of gel formation, appropriate measurement of the adhesive stiffness or viscosity approaching cured state is difficult due to increasing load transfer and subsequent shear deformation of the wooden substrate. In the case of the PUR adhesive, the apparent modulus in the cured condition is further reduced due to the emerging CO_2 bubbles.

Curing MUF on pristine wood requires a significantly longer (+33% on average, p < 0.04) duration to reach the gel time with $t_{gel} = 5.0 \pm 0.3$ h (arithmetic mean $\pm$ standard deviation) compared to measurements on extracted birch of $t_{gel} = 3.8 \pm 0.7$ h (Fig. 4A). In contrast, the gel time of PUR is $t_{gel} = 1.0 \pm 0.1$ h on pristine and extracted wood specimens
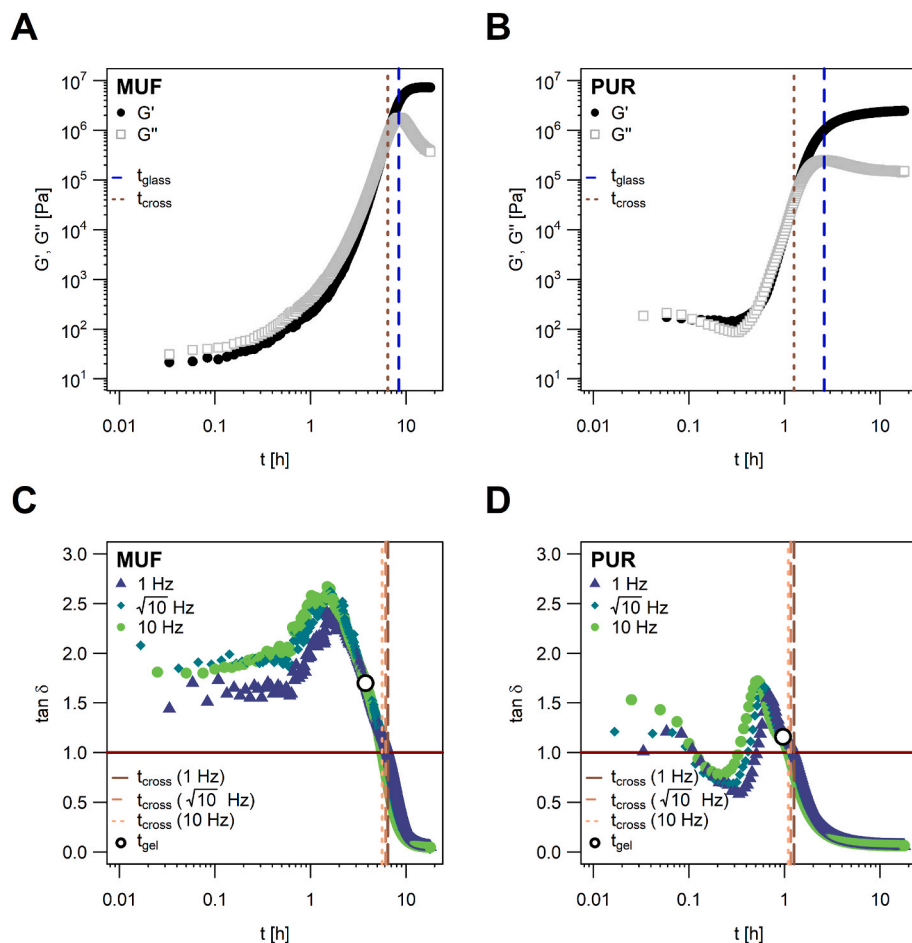
Fig. 3. Isothermal time-sweep experiment at 20 °C/65%-RH during the curing process of MUF and PUR adhesives without added extractives on extracted birch wood: A/B: Storage G' and loss G" modulus at 1 Hz showing the crossover time (t_{cross}) and the vitrification time (t_{glass}) for (A) MUF and (B) PUR adhesive. C/D: Loss factor $\tan \delta$ and crossover times (t_{cross}) at different frequencies:1 Hz (long dashed line, triangle) $\sqrt{10}$ Hz (dashed line, rhombus), 10 Hz (dotted line, filled circle) and the gel time (t_{gel}) via the local minimum of the loss factor variance (black circle) for (C) MUF and (D) PUR adhesives.
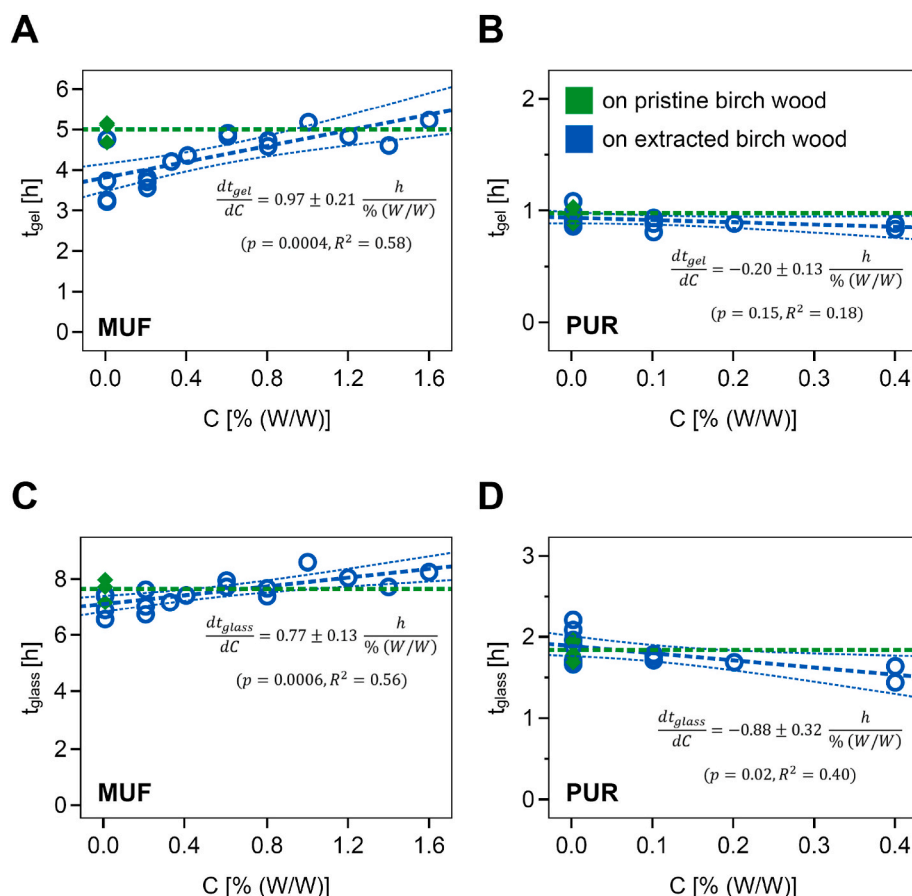
Fig. 4. Evaluation results of rheological experiments with MUF and PUR adhesives on pristine (filled green diamonds) and cold-water extracted (empty blue circles) birch wood substrate. A) MUF and B) PUR gel time t_{gel}, and C) MUF and D) PUR vitrification time t_{glass} as a function of the added extractives concentration. The blue lines are the linear regression of measurements on extracted birch wood with a confidence interval of 95%. The green dashed horizontal line indicates the average measurement result on pristine wood without added extractives in the adhesive.

alike (Fig. 4B). The vitrification time of MUF is $t_{glass} = 7.7 \pm 0.4$ h vs. 7.1 $\pm$ 0.4 h, and in the case of PUR, $t_{glass} = 1.8 \pm 0.1$ h vs. 1.9 $\pm$ 0.2 h on pristine wood vs. extracted wood, respectively, indicating no effect of the wood extract from pristine birch wood plates on the curing rate during further cross-linking of PUR. Since the adhesive transforms to a solid after gelation, the resulting severely limited mobility of the molecules results in lower effects on the vitrification time compared to the time to reach the gel formation, as seen clearly with the MUF adhesive.

Adding 0–1.6% (W/W) extractives to MUF and measuring the curing process on extracted wood plates increases both the gel time and the vitrification time by $dt_{gel}/dC = 1.0 \pm 0.2$ h/% (W/W) (Fig. 4A; p < 0.0005) and $dt_{glass}/dC = 0.8 \pm 0.2$ h/% (W/W) (Fig. 4C; p < 0.0006, respectively (slope $\pm$ standard error), as indicated by the positive slope of both curves. This can result from reacting with the lignocellulosic moieties in the extractives that reduce the reactivity of the adhesive and introduce defects in the polymer network [71]. In the case of PUR, the gel time is slightly affected, while vitrification time is reduced more, as observed by the slope values of $dt_{gel}/dC = -0.20 \pm 0.13$ h/% (W/W) (Fig. 4B; p < 0.15) and $dt_{glass}/dC = -0.9 \pm 0.3$ h/% (W/W) (Fig. 4D; p < 0.02). The slightly faster curing of PUR adhesive can be due to the acidic compounds acting as catalysts.

The viscosity gel point (time at $\eta^* > 100$ Pa s, measured at 1 Hz) is $t_\eta = 1.0–1.2$ h and 0.5–0.6 h for MUF and PUR adhesive, respectively, not significantly affected by the extractive concentration or substrate type.

This observed reactivity reduction of MUF due to the extractives can be explained by the introduction of extractive molecules that react to the adhesive oligomers and formaldehyde. Moreover, while the functional component in the hardener is a strong acid (formic acid, pKa = 3.7), the extractives weak acid compounds and minerals might act as a buffer and increase the pH of the mixture [72]. Furthermore, aliphatic and aromatic alcohols might spontaneously react with the hardener's formic

acid, forming esters [73] and thereby reducing acidity.

Acidic compounds of the extractives can catalyze the curing of PUR [74]. However, the low solubility of the polar extractives compounds, the higher initial viscosity and the generally faster curing behavior of PUR adhesive (24 Pa s, [75]) compared to water-born MUF (2–3.5 Pa s, [76]) diminish potential effects. Therefore, PUR curing dynamics were only impacted due to forced extractives addition but not in the case of pristine wood substrates. While the duration to reach the gel time remained comparatively constant, the duration to reach the glassy state at $t_{glass} = 1.8$ h was reduced upon the extractives' addition. This indicates an increased curing rate in the presence of extractives, which can be caused by acidic catalysis. An additional cross-linking with polyol compounds in the extractive cannot be excluded, but is not supported by the FTIR analysis and the mechanical measurements described below.

The MUF gap size during curing was adjusted for zero axial pressure to accommodate the imbibition of the water fraction. The solid content of the MUF formulation used is around 60%, which gives a theoretical bond line thickness in the cured state of 188 μm, assuming a moisture content of MUF in standard conditions (20 °C/65% RH) of 6% (W/W) [52]. Following the adhesive gap size reduction during MUF curing, the decrease is also slighter on pristine than extracted wood plates, correlating with gel time and vitrification parameters (Figs. SI–20A).

This effect, however, might be inverted when gluing wood with pressure since a lower viscosity increase will allow for increased adhesive flow in the pore structure under the applied pressure. For PUR measurements, the gap was kept constant to minimize the expansion of cavities (bubbles) due to CO_2 formation. This leads to an axial pressure increase on the plates of 2–3 kPa in the first 5 min of curing, which then relaxes to 1–2 kPa. At around 20 min, the CO_2 pressure is mostly released (Figs. SI–20B), independent of extractives concentration. This process coincides with the temporary crossover of G' and G", indicating

it is a result of this physical pressure effect.

3.4. Mechanical characteristics of cured adhesive films

Uniaxial tensile stress-strain measurements (UTSS) on rectangular film specimens were conducted with a universal test machine to investigate the influence of the presence of extractives on the mechanical properties of cured adhesives. This was done to assess the extractives' impact on bond lines in engineered wood products (EWPs).

Pure MUF and PUR adhesive films yielded a modulus of elasticity of $E = 2.9 \pm 0.2$ (average $\pm$ standard deviation) and 1.0 ± 0.05 GPa, a tensile strength of $\sigma_t = 21 \pm 4$ and 29 ± 2 MPa, yield stress of $\sigma_{el} = 21 \pm 4$ and 19 ± 1 MPa, and an elastic strain limit of $\varepsilon_{el} = 0.9 \pm 0.2$ and $2.1 \pm 0.1\%$, respectively.

The tensile tests on the cured film specimens indicate softening effects on both types of adhesives upon adding extractives. As shown in Fig. 5, the modulus of elasticity E, the tensile strength σ_t, the yield stress σ_{el} and the elastic strain limit ε_{el} of PUR and MUF films were negatively correlated with extractives concentration ($p < 0.0001$ in all cases, except $p = 0.0012$ for ε_{el} of MUF). The results indicate that extractives affect the mechanical properties of both polymer networks studied by softening the material, reducing the tensile strength and causing failure at slightly lower strain levels. In the case of MUF adhesive, the gradients of linear regressions are for the stiffness $dE/dC = -0.44 \pm 0.05$ GPa/% (W/W) (slope$\pm$standard error), elastic strain limit $d\varepsilon_{el}/dC = -0.22 \pm 0.06\%/\%$ (W/W), elastic stress limit (proof stress) $d\sigma_{el}/dC = -8.9 \pm 1.4$ MPa/% (W/W), and tensile strength $d\sigma_t/dC = -8.8 \pm 1.4$ MPa/% (W/W). In the case of PUR adhesive, the respective gradients are for the stiffness $dE/dC = -1.3 \pm 0.3$ GPa/% (W/W), elastic strain limit $d\varepsilon_{el}/dC$ $= -0.2 \pm 0.1\%/\%$ (W/W), elastic stress limit (proof stress) $d\sigma_{el}/dC = -10.4 \pm 2.0$ MPa/% (W/W) and tensile strength $d\sigma_t/dC = -17.0 \pm 3.4$ MPa/% (W/W)).

The mechanical effects of extractives on MUF cured adhesive films can be explained physically due to impurities taking up space, or chemically by the partial depletion of the formaldehyde fraction by reaction with phenolic compounds or incorporation of glycosides in the matrix that increase the segmental molecular weight and disturbing the regularity of the polymer matrix.

In case of PUR films, the effects can be explained also either physically by the introduction of impurities acting as plasticizers, or due to the chemical integration of polyols in the form of chain-extenders or chain-ends rather than cross-linking (due to the high viscosity of the mixture).

The stress-strain curves analyzed here, are shown in Figs. SI–21. While R^2 is around 0.3–0.5 for E, σ_t and σ_{el}, it is low for ε_{el} with $R^2 \approx 0.1$. This indicates a small effect size on the elastic strain in relation to the variance of the results as introduced by methodological effects regarding the measurement, the sample homogeneity or the method of determining ε_{el} via plastic strain estimation (proof stress method).

While there were no prior studies on extractives impacts on adhesive films available, the presented results for E of pure adhesive films are in good agreement with similar investigations of Kläusler et al. [77] on the same adhesives. In this paper, also similar tensile strength values were reported for PUR (24 MPa) but higher values of 40 MPa for MUF, possibly due to a more complex, shouldered specimen geometry, which was omitted for the purpose of the presented study. While a softer adhesive is usually considered to support bond strength in TSS measurements by reducing stress peaks [78], the lower tensile strength of the
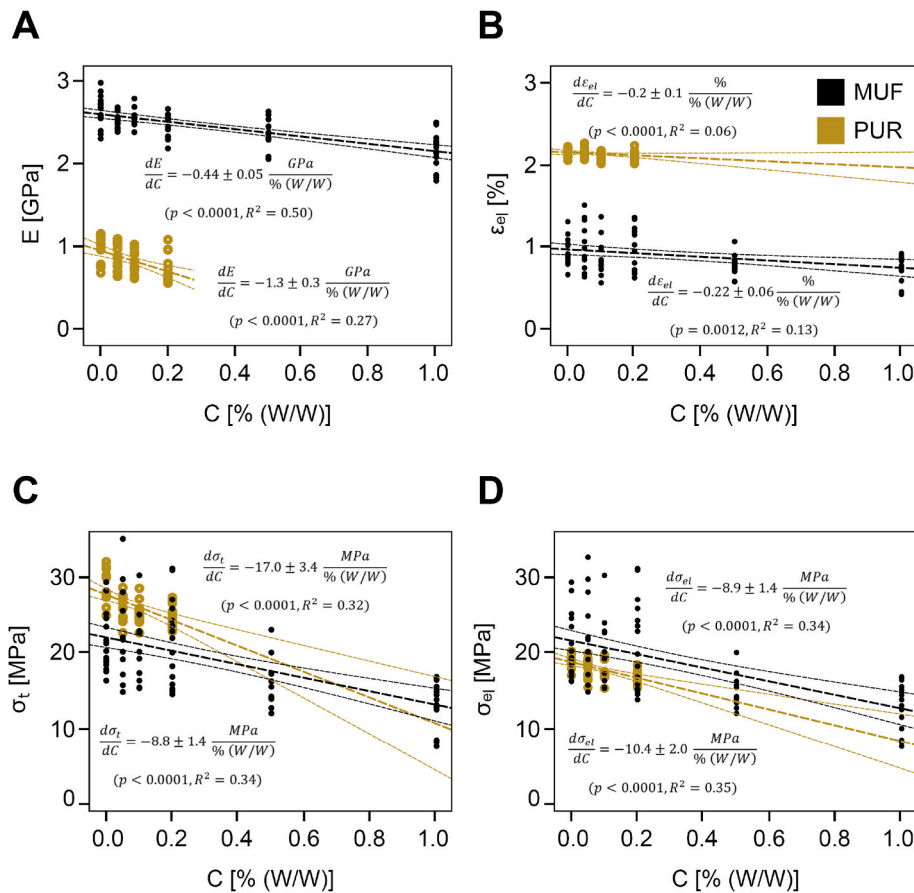

Fig. 5. Uniaxial tensile stress-strain measurements (UTSS) on adhesive films of MUF (black) and PUR (yellow) with varying concentrations C (% (W/W)) of added water-soluble extractives from birch wood, measured in equilibrium conditions of 20 °C/65%-RH after 100 d of post-curing: Dashed lines are linear regressions with 95% confidence bands).

adhesive films is expected to negatively affect TSS if cohesive or adhesive failures occur in the bond line.

Despite the softening, as seen in the tensile measurements, adding extractives did not significantly lower glass transition temperatures (T_g) as evaluated by Thermo-Mechanical Analysis (TMA). MUF adhesive films exhibit T_g values of 70–80 °C, while the variance is methodically caused since the highly-crosslinked network show only minor temperature-dependent softening reactions. T_g of PUR is in the range of 45–50 °C. Results of T_g for concentrations of extractive added can be found in Figs. SI–22.

The results of both the tensile stress-strain measurement method as well as TMA were verified by Dynamic Mechanical Analysis (DMA). T_g values for PUR and MUF by DMA of 49 °C and 63 °C, based on loss modulus peak in the temperature sweep (Figs. SI–23, right), are in good agreement with the TMA results. The average modulus of elasticity for MUF and PUR of 2.6 GPa and 1.0 GPa, as measured with stress-strain experiments on films, is also in good agreement with the frequency sweep results at 65%-RH (Figs. SI–23, left, in red).

3.5. Tensile shear strength experiments

The influence of extractives in birch wood on the mechanical performance of bond lines is of particular interest to assess the relevance and efforts of possible mitigation methods and understand the relationships between extractive-adhesive interactions during bonding and the resulting performance properties. Therefore, standard tensile shear strength (TSS) measurements [55] with pristine and extracted birch wood were conducted and compared. Statistical analysis showed no outliers [79] in strength within the measured sample groups.

For all treatment procedures on wood specimens bonded with MUF, the extracted wood specimens' average tensile shear strength values were $TSS_{extr,A1}^{MUF} = 10.7 \pm 1.7$ MPa, $TSS_{extr,A2}^{MUF} = 8.2 \pm 1.5$ MPa, $TSS_{extr,A4}^{MUF} = 7.4 \pm 1.7$ MPa and $TSS_{extr,A5}^{MUF} = 12.0 \pm 2.2$ MPa, which correspond to 7%, 19%, 14% and 13% higher average values, respectively, than those of pristine wood specimens ($TSS_{pris,A1}^{MUF} = 9.6 \pm 1.0$ MPa, $TSS_{pris,A2}^{MUF} = 6.7 \pm 1.3$ MPa, $TSS_{pris,A4}^{MUF} = 6.7 \pm 1.0$ MPa and $TSS_{pris,A5}^{MUF} = 10.7 \pm 1.3$ MPa).

In the case of PUR-bonded specimens, the average tensile shear strength increased by 11% for the A1 treatment after extraction ($TSS_{extr,A1}^{PUR} = 12.5 \pm 2.8$ MPa vs. $TSS_{pris,A1}^{PUR} = 11.3 \pm 1.7$) and remained mostly equal (±3%) when measured after post-bonding water treatments A2, A4 and A5 (MPa $TSS_{extr,A2}^{PUR} = 7.0 \pm 2.4$ MPa vs. $TSS_{pris,A2}^{PUR} = 6.8 \pm 1.7$ MPa; $TSS_{extr,A4}^{PUR} = 6.2 \pm 2.1$ MPa vs. $TSS_{pris,A4}^{PUR} = 6.3 \pm 1.0$ MPa; $TSS_{extr,A5}^{PUR} = 11.7 \pm 2.1$ MPa vs. $TSS_{pris,A5}^{PUR} = 11.4 \pm 2.0$ MPa).

As a reference, specimens from pristine solid birch wood without bond line were tested after A1 and A4 treatment, giving $TSS_{pris,A1}^{SW} = 12.7 \pm 3.0$ MPa, and $TSS_{pris,A4}^{SW} = 7.3 \pm 1.9$ MPa, respectively. Boxplots of TSS for all specimen groups are shown in Fig. 6, together with the average the wood failure percentage (WFP). Statistics on the TSS experiments and ANOVA analysis results are shown in Tables SI–6.

The variance analysis of the results indicates a significant difference between extracted wood specimens and pristine wood specimens for MUF with treatments A1 (+11%, p < 0.03), A2 (+22%, p < 0.01) and A5 (+12%, p < 0.05). The observed 11% increase of average tensile shear strength in specimens bonded with PUR and A1 treatment was insignificant with p = 0.13 (high p-values for A2, A4, and A5). The post-bonding water treatments neither significantly reinforce nor diminish the measured effect on TSS due to extraction in the case of MUF.

The extraction procedure positively affected the ultimate tensile shear stress value when using the MUF adhesive. The WFP distribution of the MUF specimens showed that the failure originates primarily within the wooden substrate for both specimens with pristine wood (average $WFP_{pris,A1}^{MUF} = 99\%$, $WFP_{pris,A2}^{MUF} = 100\%$, $WFP_{pris,A4}^{MUF} = 82\%$, and $WFP_{pris,A5}^{MUF} = 94\%$) and extracted wood (average $WFP_{extr,A1}^{MUF} = 100\%$, $WFP_{extr,A2}^{MUF} = 100\%$, $WFP_{extr,A4}^{MUF} = 89\%$, and $WFP_{extr,A5}^{MUF} = 93\%$). This further complicates the attribution of strength differences to the bond properties. The average wood failure percentages of the specimens with PUR adhesive are $WFP_{pris,A1}^{PUR} = 100\%$, $WFP_{pris,A2}^{PUR} = 37\%$, $WFP_{pris,A4}^{PUR} = 46\%$, and $WFP_{pris,A5}^{PUR} = 93\%$ for pristine wood and $WFP_{extr,A1}^{PUR} = 92\%$, $WFP_{extr,A2}^{PUR} = 30\%$, $WFP_{extr,A4}^{PUR} = 46\%$, and $WFP_{extr,A5}^{PUR} = 95\%$ for extracted wood. Comparing WFP for pristine and extracted wood specimens does not indicate changes in the failure mode of the bond lines.

When evaluating the overall ratio of specimens meeting the minimum TSS values [80,81], which are defined in the European standard for testing of adhesives using beech wood (red dotted lines in Fig. 6), an increase from 76% to only 78% in case of PUR is observed and a more pronounced increase from 65% to 85% in the case of MUF, indicating that the amount of extractives in birch wood can have an impact when used for testing waterborne adhesives like MUF.

The observed extractives effects on TSS are different from prior studies by Bockel et al. [9], where adding high concentrations of beech extractives model substances, e.g., aldehydes, terpenes, starch and carboxylic acids, on the wood surface all yielded in increased TSS for PUR, when testing in A1 conditions. In the same study, MUF specimens were not affected in A1 conditions but saccharide application (starch) diminished TSS in A4 conditions. Direct comparisons are, however, difficult due to the methodological differences.

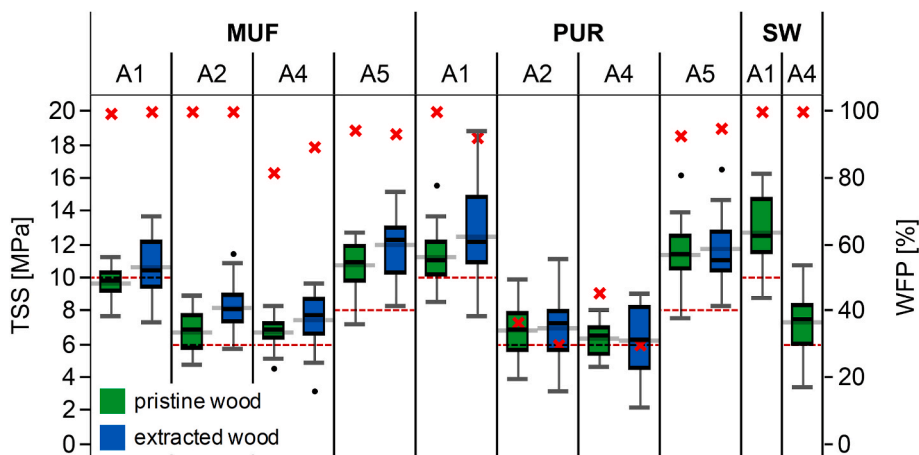In conclusion, despite using defined parameters for wood sampling,

Fig. 6. Distribution of tensile shear strength (TSS, left axis) of birch wood tensile shear specimens (EN 302–1) from pristine (green boxes, left in columns) and extracted (blue boxes, right in columns) silver birch wood bonded with MUF and PUR and solid wood specimens (SW i.e. without bond line) after different specimen treatments (A1: 20 °C/65%-RH; A2: A1 plus 4 d in water at 20 °C; A4: A1 plus 6 h in boiling water and 2 h in water at 20 °C; A5: A1 plus 6 h soaking in boiling water, 2 h in water at 20 °C and reconditioned at 20 °C/65%-RH). The average WFP (right axis) is shown as red crosses. Grey lines indicate the average TSS. Red dashed lines indicate the threshold values for standard testing according to EN 301 for MUF and EN 15425 for PUR (with beech wood, thin bond lines, type I).

conclusions on to which extent the observed strength increases are caused by the extraction treatment or other inhomogeneities in the wood remain unclear. If any, only minor effects, possibly due to a chemical weak boundary layer on the wood-adhesive interfaces, occur with birch wood and PUR adhesives. Higher differences due to the extraction procedure on TSS specimens bonded with MUF indicate an additional release and diffusion of extractives from the cell wall tissue due to their solubility with the water fraction of the adhesive.

The effect of extraction on the mechanical properties of the bond line and interphase formation by adhesive penetration should be investigated further to increase the understanding of how these effects are related to shear strength. Finally, to better understand the effects of extraction treatments on glueability, the possible impacts on the bulk wood properties should also be considered, as water-related properties, surface energy and even bio-polymer conformations might be altered by the procedure and the removal of hydrophilic compounds.

4. Conclusions

This study investigated the effects of hydrophilic extractives in birch wood (*Betula pendula* Roth) on the curing behavior, the mechanical properties of two structural wood adhesives and the tensile shear strength of bond lines.

The applied chemical analysis methods on the extractives via GC-MS, LC, UHPLC-ESI-TOF-MS measurements, as well as FTIR experiments on cured films of adhesives-extractives mixtures, provided detailed insight into the chemical composition of the extractable compounds in birch wood. The presence of mainly phenolic glycosides and fatty acids and their conjugates and, to a lower extent, saccharides, glycolipids, glycerolipids, polyphenols/lignans, and phenolics was shown.

The presence of these extractives reduced the reactivity of MUF, resulting in longer durations to reach the gel time during the curing process. This was observed by comparing curing on pristine ($\bar{t}_{gel} = 5.0\pm$ h) vs. extracted wood ($\bar{t}_{gel} = 3.8\pm$ h) plates, as well as by introducing controlled extractives concentrations ($\bar{t}_{gel} = 5.0\pm$ h – average value reached on extracted birch wood when adding $\sim 1.3\%$ (W/W) extractives in the MUF adhesive). In the solid phase, however, the delay in curing to reach a glassy state was lower, indicating that the prolonging effect of extractives was limited to the early curing stage. This could be explained due to chemical changes of the reactive MUF molecules when reacting with the water-soluble extractives (aromatic compounds), reducing the reactivity and introducing defects in the MUF polymer network.

While an increased curing speed with shorter durations to reach a glassy state was observable when adding extractives to the adhesive, no change in curing behavior was found when comparing PUR adhesive applied to pristine vs. extracted wood plates. This reflects the low compatibility/miscibility of amphiphilic/hydrophilic extractives with the hydrophobic PUR adhesive.

The uniaxial tensile stress-strain (UTSS) measurements on cured adhesive films showed a softening and weakening effect due to the presence of hydrophilic extractives of birch wood on both PUR and MUF adhesives. Meanwhile, TMA measurements on cured adhesive films did not reveal considerable changes in T_g for both adhesive types due to varying extract concentrations. Temperature- and frequency-sweep DMA experiments indicate the thermal and frequency behavior of such cured adhesives, where the elastic modulus and T_g match well the results obtained from UTSS and TMA measurements.

Tensile shear strength (TSS) measurements on lap joint specimens under different treatments demonstrated an increased average bond strength when gluing with MUF after water extraction of the birch wood: The TSS values increased by 7%–19% indicating that the presence of extractives decreases the bond line performance of waterborne adhesives. This indicates that chemical and physical interactions of the extractives with the reactive adhesive molecules, as demonstrated

experimentally, are responsible for these effects.

For specimens bonded with PUR, the TSS measurement campaign did reveal inconclusive results comparing pristine and extracted wood as adherend, with an increase for the A1 specimen treatment but no significant difference in averages in the case of the specimen water treatments A2, A4 and A5. The lower impact of the presence of extractives on TSS in the case of PUR adhesive correlates well with the rheological results. Therefore we interpret that water-soluble extractives do not interfere chemically with the PUR adhesive molecules, but physically by plasticizing the polymer network when introduced during the films preparation as shown in UTSS experiments.

The results allow to conclude that effects of hydrophilic extractives in birch wood as a raw material for EWPs can safely be disregarded when using PUR for bonding, as neither bond strength nor curing behavior were affected in a considerable way. However, an unwanted increase in reactivity might be of issue, when PUR formulations with significantly lower catalyst concentration are used. When bonding EWPs with MUF, however, prolonged processing times for bonding could result, which may be offset by adjusting the acidic catalyst concentration in the hardener component. The TSS bonding performance indicated no substantial concerns for the usage of MUF.

The current study is limited to specific adhesive types as well as formulations. Extending the scope to other resin-to-hardener ratios or formaldehyde concentrations in the case of the MUF, and adhesive catalyst concentrations in PUR adhesives can reveal adaptive optimizations to offset the extractives' effects on curing dynamics or reduce their sensitivity. A comparative analysis including other potentially interesting and already established wood species can improve the assessment of the practical relevance of the measurement results. In addition, further studies should be carried out, extending the scope by taking into account lipophilic extractives.

Submission declaration

This article has not been published previously and is not under consideration for publication elsewhere. Its publication is approved by all authors and the responsible authorities where the work was carried out. If accepted, this work will not be published elsewhere, including electronically in the same form, in English or any other language, without the copyright-holder's written consent.

Author contributions

M.E. designed the study, performed experimental work, analyzed the data and wrote the manuscript. T.B. assisted in the experimental work and revised the manuscript. M.G. supervised the untargeted metabolomics UHPLC measurements. C.M. processed untargeted metabolomics data. V.S. and W.S. conducted the DMA measurements. K.R. supervised the study, contributed to the discussion of the results and manuscript polishing. A.S.F. designed the study, analyzed data, supervised the experimental work and contributed to the writing of the manuscript.

Declaration of competing interest

The authors declare that they have no known competing financial interests or personal relationships that could have appeared to influence the work reported in this paper.

Data availability

Data will be made available upon reasonable request.

staff Andreas Tenz, Claudia Strobel and Snežana Šajkaš Sajdl for their exceptional support in the analytical chemistry laboratories (extraction procedures, IR spectrometry, LC sugar analysis and GC-MS analysis) of Holzforschung München (Technical University of Munich). We also thank the staff of Holzforschung München – and, especially, Frank Moosmann and Roland Braun – for their continuous and unconditional support in our research activities.

Supplementary data

Supplementary data to this article can be found online at https://doi.org/10.1016/j.ijadhadh.2023.103447.

References

[1] Roitto M, Siwale W, Tanner J, Ilvesniemi H, Julkunen-Tiitto R, Verkasalo E. Characterization of extractives in tree biomass and by-products of plywood and saw mills from Finnish birch in different climatic regions for value-added chemical products. In: *International scientific Conference on hardwood processing proceedings, québec city. Canada; Sep.* 2015. p. 174–81.

[2] Finnish Forest Industries Federation. In: Handbook of Finnish plywood. Lahti: Kirjapaino Markprint Oy; 2007.

[3] Cakiroglu EO, Demir A, Aydin I. Comparison of birch and beech wood in terms of economic and technological properties for plywood manufacturing. Drv Ind Jun. 2019;70(2):169–74. https://doi.org/10.5552/drvind.2019.1828.

[4] Jeitler G, Augustin M. "Is Birch the better Beech? Grading, processing and mechanical properties of birch Glulam and birch CLT (Ist Birke die bessere Buche? Mechanische Eigenschaften und Referenzprojekte aus BIRKE|BSH&BSP)," Garmisch. 2016 [Online]. http://www.forum-holzbau.com/pdf/48_IHF_2016_Jeitler.pdf. [Accessed 15 April 2020].

[5] Ohnesorge D, Henning M, Becker G. Review: relevance of hardwoods for the production of glued laminated timber: survey among GLT-manufacturers in Germany, Austria and Switzerland (Review: bedeutung von Laubholz bei der Brettschichtholzherstellung: befragung unter BSH-Produzenten in Deutschland,Österreich und der Schweiz). Holztechnologie 2009;50(6):47–9.

[6] Konnerth J, Kluge M, Schweizer G, Miljković M, Gindl-Altmutter W. Survey of selected adhesive bonding properties of nine European softwood and hardwood species. Eur. J. Wood Prod. 2016;74(6):809–19. https://doi.org/10.1007/s00107-016-1087-1. Nov.

[7] Hse C, Kuo M. Influence of extractives on wood gluing and finishing: a review. For Prod J 1988;38:52–6.

[8] Roffael E. Significance of wood extractives for wood bonding. Appl Microbiol Biotechnol 2016;100(4):1589–96. https://doi.org/10.1007/s00253-015-7207-8. Feb.

[9] Bockel S, et al. The role of wood extractives in structural hardwood bonding and their influence on different adhesive systems. Int J Adhesion Adhes 2019;91:43–53. https://doi.org/10.1016/j.ijadhadh.2019.03.001. Jun.

[10] Chen CM. Effect of extractive removal on adhesion and wettability of some tropical woods. For Prod J 1970;20(1):36–41.

[11] Kuo M-L, Dicarlo D, Hse C-Y. Influence of extractives on bonding properties of white and southern red oak. J Adhes Apr. 1984;16(4):257–77. https://doi.org/10.1080/00218468408074922.

[12] Roffael E, Rauch W. Extractives in Oak and their Influence on the Glueability with Alkaline Phenol Formaldehyde Resins (Extraktstoffe in Eiche und ihr Einfluß auf die Verleimbarkeit mit alkalischen Phenol-Formaldehydharzen). Holz als Roh-und Werkstoff May 1974;32(5):182–7. https://doi.org/10.1007/BF02607288.

[13] Wang Y-S. Influence of extractives on bonding properties of white oak," Dissertation. Ames: Iowa State University; 1992. https://doi.org/10.31274/rtd-180813-9568.

[14] Narayanamurti D, Gupta RC, Verma GM. Influence of wood extractives on the rheological properties of casein-NaOH-water system. Appl Sci Res 1964;12(4–5):340–8. https://doi.org/10.1007/BF03185006. Jul.

[15] Özparpucu M, Wolfrum T, Windeisen-Holzhauser E, Knorz M, Richter K. Combined FTIR spectroscopy and rheology for measuring melamine urea formaldehyde (MUF) adhesive curing as influenced by different wood extracts. Eur. J. Wood Prod. 2020;78(1):85–91. https://doi.org/10.1007/s00107-019-01481-0.

[16] Özparpucu M, et al. Acidic wood extractives accelerate the curing process of emulsion polymer isocyanate adhesives. J Appl Polym Sci Jun. 2022;139(21):52189. https://doi.org/10.1002/app.52189.

[17] Yoshimoto T. Effect of extractives on the utilization of wood. In: Rowe JW, editor. Natural products of woody plants. In springer series in wood science. Berlin, Heidelberg: Springer Berlin Heidelberg; 1989. p. 920–31. https://doi.org/10.1007/978-3-642-74075-6_24.

[18] Arnold RG, Nelson JA, Verbanc JJ. Recent advances in isocyanate chemistry. Chem Rev Feb. 1957;57(1):47–76. https://doi.org/10.1021/cr50013a002.

[19] Kägi A, Niemz P, Mandallaz D. Influence of moisture content and selected technological parameters on the adhesion of one-part polyurethane adhesives under extreme climatical conditions (Einfluss der Holzfeuchte und ausgewählter technologischer Parameter auf die Verklebung mit 1K-PUR Klebstoffen unter extremen klimatischen Bedingungen). Holz Roh Werkst 2006;64(4):261–8. https://doi.org/10.1007/s00107-005-0088-2. Aug.

[20] Shkapenko George, Gmitter GT, Gruber EE. Mechanism of the water-Isocyanate reaction. Ind Eng Chem Jul. 1960;52(7):605–8. https://doi.org/10.1021/ie50607a031.

[21] Bomba J, Sedivka P, Böhm M, Devera M. Influence of moisture content on the bond strength and water resistance of bonded wood joints. Bioresources Sep. 2014;165:5208–18. https://doi.org/10.15376/biores.9.3.5208-5218.

[22] Witt M. Novel plate rheometer configuration allows monitoring real-time wood adhesive curing behavior. J Adhes Sci Technol Jan. 2004;18(8):893–904. https://doi.org/10.1163/156856104840534.

[23] Schmidt M, Knorz M, Wilmes B. A novel method for monitoring real-time curing behaviour. Wood Sci Technol Aug. 2010;44(3):407–20. https://doi.org/10.1007/s00226-010-0359-x.

[24] Bockel S, et al. Influence of wood extractives on two-component polyurethane adhesive for structural hardwood bonding. J Adhes 2018;94(10):829–45. https://doi.org/10.1080/00218464.2017.1389279. Aug.

[25] Künninger T, Fischer A, Bordeanu NC, Richter K. Water soluble larch extractive: impact on 1P-PUR wood bonds. In: Wood structure and properties '06: proceedings of abstracts of the 5th international symposium. Zvolen, Slovakia: Arbora publishers; 2006. p. 71–6 [Online]. Available: https://www.dora.lib4ri.ch/empa/islandora/object/empa:8415.

[26] Roffael E, Dix B, Okum J. Use of spruce tannin as a binder in particleboards and medium density fiberboards (MDF). Holz als Roh- Werkst Dec. 2000;58(5):301–5. https://doi.org/10.1007/s001070050432.

[27] Bolton AJ, Irle MA. Physical aspects of wood adhesive bond formation with formaldehyde based adhesives Part I. The effect of curing conditions on the physical properties of urea formaldehyde films. Holzforschung Jan. 1987;41(3):155–8. https://doi.org/10.1515/hfsg.1987.41.3.155.

[28] Konnerth J, Gindl W, Müller U. Elastic properties of adhesive polymers. I. Polymer films by means of electronic speckle pattern interferometry. J Appl Polym Sci Mar. 2007;103(6):3936–9. https://doi.org/10.1002/app.24434.

[29] Bergman J, Lindgren BO, Svahn CM, Mellander O, Hinton M. Triterpenes and 4alpha-methylsterols in birch wood. Acta Chem Scand 1965;19:1661–6. https://doi.org/10.3891/acta.chem.scand.19-1661.

[30] Fengel D, Wegener G. Wood: chemistry, ultrastructure, reactions. Berlin ; New York: W. de Gruyter; 1984.

[31] Piispanen R, Saranpää P. Seasonal and within-stem variations of neutral lipids in silver birch (Betula pendula) wood. Tree Physiol Sep. 2004;24(9):991–9. https://doi.org/10.1093/treephys/24.9.991.

[32] Sutela S, et al. Phenolic compounds in ectomycorrhizal interaction of lignin modified silver birch. BMC Plant Biol 2009;9(1):124. https://doi.org/10.1186/1471-2229-9-124.

[33] Hiltunen E, Pakkanen TT, Alvila L. Phenolic compounds in silver birch (Betula pendula Roth) wood. Holzforschung 2006;60(5):519–27. https://doi.org/10.1515/HF.2006.086. Aug.

[34] Sutela S, et al. Phenolic compounds and expression of 4CL genes in silver birch clones and Pt4CL1a lines. PLoS One Dec. 2014;9(12):e114434. https://doi.org/10.1371/journal.pone.0114434.

[35] Julkunen-Tiitto R, Rousi M, Bryant J, Sorsa S, Keinänen M, Sikanen H. Chemical diversity of several Betulaceae species: comparison of phenolics and terpenoids in northern birch stems. Trees (Berl) 1996;11(1):16. https://doi.org/10.1007/s004680050053.

[36] Hynynen J, Niemisto P, Vihera-Aarnio A, Brunner A, Hein S, Velling P. Silviculture of birch (Betula pendula Roth and Betula pubescens Ehrh.) in northern Europe. Forestry Jan. 2010;83(1):103–19. https://doi.org/10.1093/forestry/cpp035.

[37] Willems W. The water vapor sorption mechanism and its hysteresis in wood: the water/void mixture postulate. Wood Sci Technol May 2014;48(3):499–518. https://doi.org/10.1007/s00226-014-0617-4.

[38] McLafferty FW, Hertel RH, Villwock RD. Probability based matching of mass spectra. Rapid identification of specific compounds in mixtures. Org Mass Spectrom Jul. 1974;9(7):690–702. https://doi.org/10.1002/oms.1210090710.

[39] Fengel D, Wegener G. Hydrolysis of polysaccharides with trifluoroacetic acid and its application to rapid wood and pulp analysis. In: Brown RD, Jurasek L, editors. Hydrolysis of cellulose: mechanism of enzymatic and acid catalysis. Advances in chemistry series, no. 181. Washington, D. C.: American Chemical Society; 1979. p. 145–58. https://doi.org/10.1021/ba-1979-0181.ch007.

[40] Fengel D, Przyklenk M. Studies on kapok. 2. Chemical investigations. Holzforschung 1986;40(6):325–30.

[41] Kessner D, Chambers M, Burke R, Agus D, Mallick P. ProteoWizard: open source software for rapid proteomics tools development. Bioinformatics 2008;24(21):2534–6. https://doi.org/10.1093/bioinformatics/btn323. Nov.

[42] Smith CA, Want EJ, O'Maille G, Abagyan R, Siuzdak G. XCMS: processing mass spectrometry data for metabolite profiling using nonlinear peak alignment, matching, and identification. Anal Chem Feb. 2006;78(3):779–87. https://doi.org/10.1021/ac051437y.

[43] Tsugawa H, et al. MS-DIAL: data-independent MS/MS deconvolution for comprehensive metabolome analysis. Nat Methods 2015;12(6):523–6. https://doi.org/10.1038/nmeth.3393. Jun.

[44] Dührkop K, et al. Systematic classification of unknown metabolites using high-resolution fragmentation mass spectra. Nat Biotechnol 2021;39(4):462–71. https://doi.org/10.1038/s41587-020-0740-8. Apr.

[45] Stapf G, Zisi N, Aicher S. Curing behaviour of structural wood adhesives - parallel plate rheometer results. Pro Ligno 2013;9(4):109–17.

[46] Winkler C, Schwarz U, Senge B. Materials science analysis of the setting behavior of wood adhesives using the example of 1K-PUR (Materialwissenschaftliche Analyse des Abbindeverhaltens von Holzklebstoffen am Beispiel von 1K-PUR). Chem Ing Tech Jun. 2020;92(6):759–68. https://doi.org/10.1002/cite.201900171.

[47] Vidil T, Cloître M, Tournilhac F. Control of gelation and network properties of cationically copolymerized mono- and diglycidyl ethers. Macromolecules 2018;51 (14):5121–37. https://doi.org/10.1021/acs.macromol.8b00406. Jul.

[48] Chambon F, Winter HH. Linear viscoelasticity at the gel point of a crosslinking PDMS with imbalanced stoichiometry. J Rheol 1987;31(8):683–97. https://doi.org/10.1122/1.549955. Nov.

[49] Winter HH. Can the gel point of a cross-linking polymer be detected by the G'-G'' crossover? Polym Eng Sci Dec. 1987;27(22):1698–702. https://doi.org/10.1002/pen.760272209.

[50] Winter HH. The critical gel. In: Borsali R, Pecora R, editors. Structure and dynamics of polymer and colloidal systems. Dordrecht: Springer Netherlands; 2002. p. 439–70. https://doi.org/10.1007/978-94-010-0442-8_14.

[51] Suman K, Joshi YM. On the universality of the scaling relations during sol-gel transition. J Rheol 2020;64(4):863–77. https://doi.org/10.1122/1.5134115. Jul.

[52] Winkler C, Raskop S, Sydow S, Engelhardt M. Wood adhesives: factors influencing the determination of mechanical properties (Holzklebstoffe: Einflussfaktoren auf die Ermittlung mechanischer Kennwerte). In: Tagungsband des 20. Dresden: Holztechnologischen Kolloquiums Dresden; Apr. 2022.

[53] ISO 527-1:2019 Plastics - determination of tensile properties - Part 1: general principles. ISO; 2019 [Online], https://www.iso.org/standard/75824.html. [Accessed 16 September 2022].

[54] Ross CTF, Bird J, Little A. Mechanics of solids. third ed. London ; New York: Routledge, Taylor & Francis Group; 2022.

[55] EN 302-1:2013 Adhesives for load-bearing timber structures - test methods - Part 1: determination of longitudinal tensile shear strength. CEN; 2019 [Online], https://www.iso.org/standard/75824.html. [Accessed 16 September 2022].

[56] Wagenführ R, Wagenführ A. *Holzatlas*, 7., Überarbeitete und ergänzte Auflage. München: Hanser; 2022. https://doi.org/10.3139/9783446468399 [Online]. Available:.

[57] Sridach W, Jonjankiat S, Wittaya T. Effect of citric acid, PVOH, and starch ratio on the properties of cross-linked poly(vinyl alcohol)/starch adhesives. J Adhes Sci Technol Aug. 2013;27(15):1727–38. https://doi.org/10.1080/01694243.2012.753394.

[58] Wang X, Deng Y, Li Y, Kjoller K, Roy A, Wang S. In situ identification of the molecular-scale interactions of phenol-formaldehyde resin and wood cell walls using infrared nanospectroscopy. RSC Adv 2016;6(80):76318–24. https://doi.org/10.1039/C6RA13159J.

[59] Emmerich L, Bollmus S, Militz H. Wood modification with DMDHEU (1.3-dimethylol-4.5-dihydroxyethyleneurea) – state of the art, recent research activities and future perspectives. Wood Mater Sci Eng Jan. 2019;14(1):3–18. https://doi.org/10.1080/17480272.2017.1417907.

[60] Arora A, Lin T-S, Beech HK, Mochigase H, Wang R, Olsen BD. Fracture of polymer networks containing topological defects. Macromolecules Sep. 2020;53(17):7346–55. https://doi.org/10.1021/acs.macromol.0c01038.

[61] Ni H, Skaja AD, Soucek MD. Acid-catalyzed moisture-curing polyurea/polysiloxane ceramer coatings. Prog Org Coating Dec. 2000;40(1–4):175–84. https://doi.org/10.1016/S0300-9440(00)00116-8.

[62] Lim H, Hoag SW. Plasticizer effects on physical–mechanical properties of solvent cast Soluplus® films. AAPS PharmSciTech Sep. 2013;14(3):903–10. https://doi.org/10.1208/s12249-013-9971-z.

[63] Immergut EH, Mark HF. "Principles of plasticization," in *Plasticization and plasticizer processes*. 48 Advances in Chemistry 1965;48:1–26. https://doi.org/10.1021/ba-1965-0048.ch001. AMERICAN CHEMICAL SOCIETY.

[64] Kandelbauer A, Despres A, Pizzi A, Taudes I. Testing by fourier transform infrared species variation during melamine–urea–formaldehyde resin preparation. J Appl Polym Sci Nov. 2007;106(4):2192–7. https://doi.org/10.1002/app.26757.

[65] Zhang J, Wang X, Zhang S, Gao Q, Li J. Effects of melamine addition stage on the performance and curing behavior of melamine-urea-formaldehyde (MUF) resin. Bioresources Sep. 2013;8(4):5500–14. https://doi.org/10.15376/biores.8.4.5500-5514.

[66] Socrates G. In: Infrared and Raman characteristic group frequencies: tables and charts. repr. As paperback. 3. Chichester: Wiley; 2010.

[67] Sánchez-Ferrer A, Rogez D, Martinoty P. Synthesis and characterization of new polyurea elastomers by sol/gel chemistry. Macromol Chem Phys Jun. 2010;211 (15):1712–21. https://doi.org/10.1002/macp.201000117.

[68] Sánchez-Ferrer A, et al. Polyurea networks from moisture-cure, reaction-setting, aliphatic polyisocyanates with tunable mechanical and thermal properties. ACS Appl. Polym. Mater. Aug. 2021;3(8):4070–8. https://doi.org/10.1021/acsapm.1c00578.

[69] Malucelli G, Priola A, Ferrero F, Quaglia A, Frigione M, Carfagna C. Polyurethane resin-based adhesives: curing reaction and properties of cured systems. Int J Adhesion Adhes Feb. 2005;25(1):87–91. https://doi.org/10.1016/j.ijadhadh.2004.04.003.

[70] Merline DJ, Vukusic S, Abdala AA. Melamine formaldehyde: curing studies and reaction mechanism. Polym J 2013;45(4):413–9. https://doi.org/10.1038/pj.2012.162. Apr.

[71] Böger T, Sanchez-Ferrer A, Richter K. Hydroxymethylated resorcinol (HMR) primer to improve the performance of wood-adhesive bonds – a review. Int J Adhesion Adhes Mar. 2022;113:103070. https://doi.org/10.1016/j.ijadhadh.2021.103070.

[72] Beynon RJ, Easterby JS. Buffer solutions: the basics. first ed. Taylor & Francis; 2004. https://doi.org/10.4324/9780203494691.

[73] Tarkow H, Stamm AJ. The reaction of formic acid with carbohydrates. I. The reaction of formic acid with sugars. J Phys Chem Feb. 1952;56(2):262–6. https://doi.org/10.1021/j150494a026.

[74] Schotman AHM. The reaction of isocyanates with carboxylic acids and its application to polymer synthesis. Delft, Netherlands: Delft University of Technology; 1993 [Online]. Available: http://resolver.tudelft.nl/uuid:471daa66-8607-4221-a3a6-cca967887796.

[75] Henkel & Cie AG, editor. LOCTITE® HB S309 PURBOND, technical data sheet (German). Henkel & Cie. AG Sempach Station; 2015.

[76] Türmerleim GmbH. In: Kauramin® resin 683 liquid with Kauramin® hardener 688 liquid in wood construction, technical data sheet (Kauramin® Leim 683 flüssig mit Kauramin® Härter 688 flüssig im Holzleimbau, Technisches Merkblatt). Ludwigshafen: Türmerleim GmbH; 2008.

[77] Kläusler O, Clauß S, Lübke L, Trachsel J, Niemz P. Influence of moisture on stress–strain behaviour of adhesives used for structural bonding of wood. Int J Adhesion Adhes 2013;44:57–65. https://doi.org/10.1016/j.ijadhadh.2013.01.015. Jul.

[78] Quispe Rodríguez R, de Paiva WP, Sollero P, Bertoni Rodrigues MR, de Albuquerque ÉL. Failure criteria for adhesively bonded joints. Int J Adhesion Adhes Sep. 2012;37:26–36. https://doi.org/10.1016/j.ijadhadh.2012.01.009.

[79] Grubbs FE. Procedures for detecting outlying observations in samples. Technometrics Feb. 1969;11(1):1–21. https://doi.org/10.1080/00401706.1969.10490657.

[80] EN 301:2017 Adhesives, phenolic and aminoplastic, for load-bearing timber structures - classification and performance requirements. CEN; 2017.

[81] EN 15425. Adhesives - one component polyurethane (PUR) for load-bearing timber structures - classification and performance requirements. CEN; 2017. 2017.